Determination and analysis of plasma radiative properties for numerical simulations of laboratory radiative blast waves launched in xenon clusters

R. Rodriguez[a,b,*], J. M. Gil[a,b], G. Espinosa[a], R. Florido[a,b], M. A. Mendoza[a,b], P. Martel[a,b], E. Minguez[b], D. R. Symes[c], M. Hohenberger[d], R. A. Smith[d]

[a] *Departamento de Fisica, Universidad de Las Palmas de Gran Canaria, Campus de Tafira, Las Palmas de Gran Canaria, Spain*
[b] *Instituto de Fusion Nuclear, Universidad Politecnica de Madrid. 28006 Madrid, Spain*
[c] *Central Laser Facility, Rutherford Appleton Laboratory, Oxfordshire, OX11 OQX, UK*
[d] *Blackett Laboratory, Imperial College London, SW7, 2BZ, UK*

[*] *Author for correspondence: R. Rodriguez, email: rrodriguez@dfis.ulpgc.es*
Received 13 Nov 2012; Accepted 31 Jan 2013; Available Online 31 Jan 2013

Abstract

Radiative shock waves play a pivotal role in the transport energy into the stellar medium. This fact has led to many efforts to scale the astrophysical phenomena to accessible laboratory conditions and their study has been highlighted as an area requiring further experimental investigations. Low density material with high atomic mass is suitable to achieve radiative regime, and, therefore, low density xenon plasmas are commonly used for the medium in which the radiative shocks propagate. The knowledge of the plasma radiative properties is crucial for the correct understanding and for the hydrodynamic simulations of radiative shocks. In this work, we perform an analysis of the radiative properties of xenon plasmas in a range of matter densities and electron temperatures typically found in laboratory experiments of radiative shocks launched in xenon plasmas. Furthermore, for a particular experiment, our analysis is applied to make a diagnostics of the electron temperatures of the radiative shocks since they could not be experimentally measured.

Keywords: Plasma radiative properties; Xenon plasmas; Laboratory astrophysics; Radiative shocks

1. Introduction

The fact that the hydrodynamics can be scaled correctly between laboratory and astrophysical scenarios [1-6] and also the improvement of high-power laser systems that allow us to generate plasmas that are in the regimes for certain astrophysical systems have led to the successful design of laboratory astrophysical experiments in the last two decades. These experiments offer two clear advantages: on one hand, they permit to explain and predict what occurs in astrophysical phenomena and, besides, they are repeatable and the initial conditions are under control; on the other hand, these experiments also provide important data for verification and validation of several aspects of numerical codes such as atomic physics, equation of state, radiative transfer and hydrodynamics.

Shock waves are one of the most interesting phenomena in astrophysics. They play a pivotal role in the transport of energy into the interstellar medium [7] and in addition they are ubiquitous throughout the universe. When the radiation transport is important to the total energy budget of the shock wave this can be radiatively driven and the radiative processes may then significantly alter its dynamics. At high shock velocity, the shocked medium is heated and ionized emitting radiation, which gives rise to radiative cooling. The radiation emitted in turn heats and ionizes the unshocked medium leading to the creation of a radiative precursor [8]. Radiative shocks are also common in astrophysics and they can be observed around astronomical objects in a wide variety of forms, e.g. accretion shock, pulsating stars, supernovae in their radiative cooling stage, bow shocks of stellar jet in galactic medium, collision of interstellar clouds and entry of rockets or comets into planetary atmospheres [9-11] and they are also observed in laser inertial fusion [12]. Thus, the relevance of the radiative shocks as well as the developing ability to perform radiation-hydrodynamic experiments and the need of experiments to benchmark new radiation-hydrodynamics codes useful for astrophysical simulations [13] have motivated laboratory studies of these phenomena. These codes need accurate computation of radiative properties, such as monochromatic opacities and emissivities, mean opacities and radiative power losses, in an extensive range of thermodynamic conditions. Their calculation is a complex task, overall under non-local thermodynamic conditions (NLTE), where there is no a priori expression for the calculation of the atomic level populations in the plasma and, therefore, one must use a collisional-radiative model [14]. This requires the solution of a set of rate equations, with coupling of configurations, free electrons and photons, which also entails a high computational time. These facts have led to perform LTE simulations [15, 16] to obtain the average ionization and mean opacities or to use cooling rates given by analytical formulas [17-19] which are accurate enough for low densities only. However, these approaches could give unphysical solutions.

In this work we first perform a brief analysis of some relevant radiative properties of xenon plasmas in a range of matter densities and electron temperatures typically found in radiative shocks launched in xenon clusters in laboratory. In particular, the plasma average ionization, charge state distribution (CSD), monochromatic emissivities and opacities, photon mean free paths and cooling times will be analyzed. This analysis will allow us to characterize this kind of laboratory radiative shocks. Furthermore, for a particular

experiment carried out using the THOR laser system at the University of Texas [15] we perform a diagnostics of the electron temperatures of the radiative shock since they could not be experimentally measured. In this experiment radiative blast waves are launched in a xenon plasma, that are generally described as an expanding shocks that are in the process of sweeping up the material that is ahead of the shock and which are important in astrophysical scenarios such as the supernova remnants. Next section is devoted to a brief explanation of the theoretical model employed in this work and in Section 3 the results and conclusions are presented.

2. Theoretical Model

2.1. Collisional-radiative model

Following the standard NLTE modeling approach, where an account of the existing atomic states is made and the microscopic (radiative and collisional) processes connecting these states are identified, a rate equation system describing the population density of the atomic states is built and solved, giving the population distribution. Therefore, to find the level population distribution, under stationary situations, the following system of rate equations is solved

$$\sum_{\zeta' j} N_{\zeta' j}\mathbb{R}^{+}_{\zeta' j\to\zeta i} - \sum_{\zeta' j} N_{\zeta i}\mathbb{R}^{-}_{\zeta i\to\zeta' j} = 0, \quad (1)$$

where $N_{\zeta i}$ is the population density of the atomic level i of the ion with charge state ζ. The terms $\mathbb{R}^{+}_{\zeta' j\to\zeta i}$ and $\mathbb{R}^{-}_{\zeta i\to\zeta' j}$ take into account all the atomic processes which contribute to populate and depopulate the state ζi, respectively. This set of equations constitutes the so-called collisional-radiative steady state (CRSS) model. In this work, the calculations of the plasma atomic level populations were performed using the CRSS implemented in the computational code named ABAKO. A detailed description of this work can be found elsewhere [20, 21] and in this section we will only highlight some of its aspects. In ABAKO it is assumed that the system has had enough time to thermalize and, therefore, both the electrons and ions have a Maxwell-Boltzmann type energy distribution. Furthermore, in ABAKO it is also assumed that electron and ion temperatures are equal. Therefore, in the following, the electron temperature, T_e, will be assumed as the plasma temperature. The CRSS implemented in ABAKO is applied to low-to-high Z ions under a wide range of laboratory or astrophysical plasma conditions: Coronal Equilibrium, NLTE or LTE, optically thin and thick plasmas. A special care was taken during the development of this CRSS model to achieve an optimal equilibrium between accuracy and computational cost. Hence, for the rate coefficients of the atomic processes included in the CRSS model analytical expressions have been employed, which yield a substantial saving of computational requirements, but providing satisfactory results in relation to those obtained from more sophisticated codes and experimental data as it has been proved in some of the last NLTE code comparison workshops [22-24]. The processes included in this CRSS model are the following: collisional ionization [25] and three-body recombination, spontaneous decay, collisional excitation [26] and deexcitation, radiative recombination [27], electron capture and autoionization. We have added between brackets the references where from their approximated analytical rates coefficients have been acquired. The rates of the inverse processes are obtained through the detailed balance principle. It is worth pointing out that the autoionizing states are included explicitly. It has been proved that their contribution is critical in the determination of the ionization balance. The cross section of the autoionization is evaluated using detailed balance principle from the electron capture cross section. This one is obtained from the collisional excitation cross section using a known approximation [28]. ABAKO does not include collisional processes between ions and in this paper no radiation-driven processes are explicitly considered.

In this work, the atomic data required for the CRSS model were generated using the FAC code [29]. Since in this work we are interested in low ionized Xe plasmas, the atomic calculations were carried out in the relativistic detailed configuration accounting (RDCA) approach. The continuum lowering due to the influence of the plasma surrounding is also considered. In this work, this one is calculated by means of the expression due to Stewart and Pyatt [30]. Because of the inclusion of the continuum lowering, the kinetics equations must be solved iteratively, since the atomic data depend on ionization balance. Finally, a key factor in the CRSS calculations is the choice of configurations included in the model. Including configurations with energies up to three times the ionization potential should be adequate for accurate modeling of thermal plasmas [31, 32]. A detailed statement of the configurations considered in this work can be found in [33].

2.2. Calculation of the radiative properties

In this work, the plasma radiative properties were calculated using RAPCAL computational code. A detailed description can be found in [34]. As it was made for ABAKO, in this section only some relevant aspects are commented. RAPCAL was developed to obtain several relevant plasma radiative properties such as the monochromatic absorption and emission coefficients, mean and multigroup opacities, source functions, radiative power losses, specific intensities and plasma transmission. Both the monochromatic emissivity and absorption include the bound-bound, bound-free and free-free contributions. For the bound-bound transitions we use the radiative transitions rates obtained from FAC. are calculated in the single multipole approximation, and in this work they were obtained in the electric dipole approach. The line strengths are corrected due to the configuration interaction within the same non-relativistic configurations. The line profile is the same both for the absorption and the emissivity since in this work complete redistribution hypothesis is assumed [35] and in its evaluation natural, Doppler, electron-impact [36] and unresolved transition array (UTA) [37] broadenings are included. The line-shape function is applied with the Voigt profile that incorporates all these broadenings. Due to, for the plasma conditions analyzed in this work, Xe is lowly ionized, line contribution is the most relevant one to the spectra and for this reason the photoionization cross section for bound-free transitions has been evaluated using the semiclassical expression of Kramers [27]. Finally, for the free-free contributions to the emissivity and the absorption the Kramers semi-classical expression for the inverse bremsstrahlung cross section has been used [38]. Furthermore, in order to determine the opacity, it is also taken into account the absorption due to the scattering of photons. In RAPCAL this one is approximated using the Thomson scattering cross section [39]. From the monochromatic opacities the Planck and Rosseland

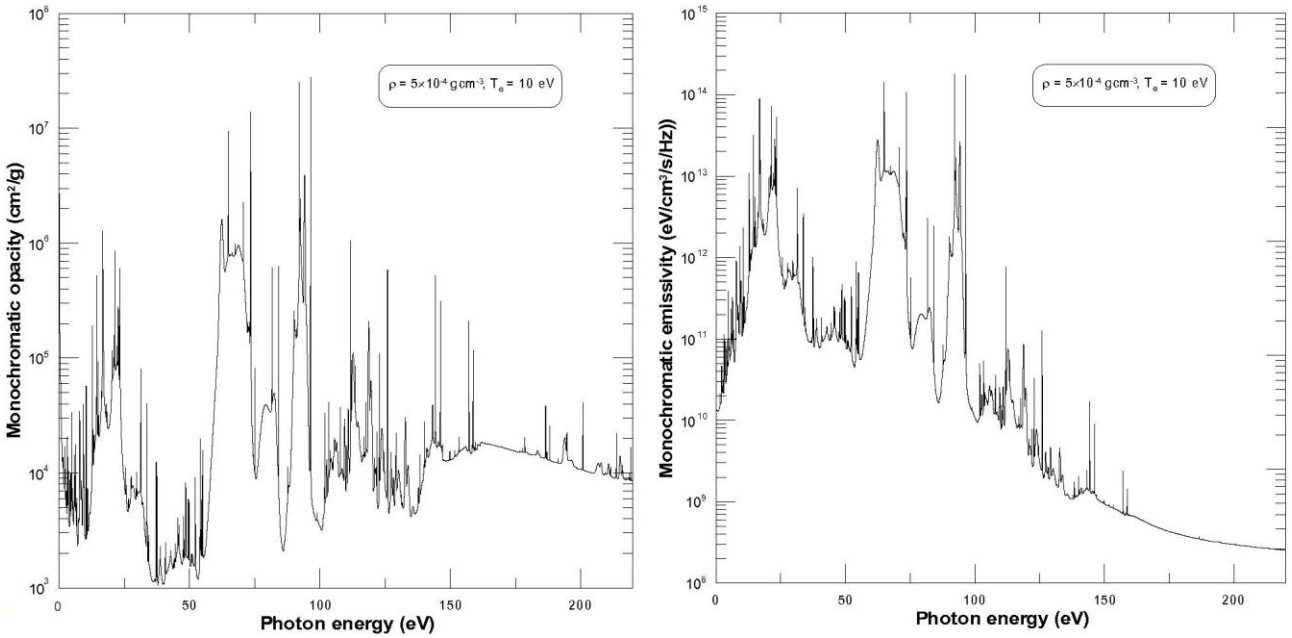

Figure 1. Monochromatic opacity and emissivity for a density of matter of 5×10^{-4} gcm $^{-3}$ and at an electron temperature of 10 eV.

mean opacities are calculated [40]. The radiative power loss, another radiative property of interest in this work is obtained according to [41] and it also includes bound-bound, bound-free and free-free contributions.

3. Results and Discussion

This section is divided into two subsections. In the first one we present a brief comment of the average ionization and charge state distribution, i.e. the fractional abundance of each ion in the plasma, of xenon plasmas for matter densities and electron temperatures ranged between $10^{-5} - 10^{-3}$ gcm $^{-3}$ and $1 - 20$ eV, respectively, which are the ones typically found in blast waves launched in cluster of gases. Furthermore, we also present some comments on the optical and radiative character of these blast waves. Further explanations of these issues can be found in [33]. The second subsection is devoted to the diagnostics of the electron temperatures of radiative blast waves launched in a xenon cluster in laboratory using the THOR laser at the University of Texas [15]. We also checked the asseverations made in the first subsection regarding the optical and radiative character for the blast waves of this experiment in particular.

3.1. Characterization of the blast waves launched in xenon and analysis of the average ionization and charge state distribution

In [33] the average ionization map of Xe in the range of plasma conditions commented above was presented. The degree of ionization, which is calculated as

$$\overline{Z} = \frac{n_e}{n_{ion}} \tag{2}$$

where n_e and n_{ion} are the electron and ion number densities, respectively, is a key quantity since, for example, it is needed to obtain the plasma thermodynamic properties and, besides, its knowledge permits a subsequent optimization in the computation of level populations and radiative properties since it reduces the number of ions to include in the calculations. In that work, it was concluded that for the conditions under study the degree of ionization of Xe plasmas is low, always lesser than 10. This low ionization justifies the RDCA approach employed for the atomic model. In [33] it was also analyzed the plasma charge state distribution (CSD), which is defined as the set of the population densities of the ions present in the plasma for a given condition of density and temperature, obtained from the resolution of the rate equations. The analysis was made for the range of temperatures of 1-20 eV and for a density of matter of 5×10^{-4} gcm $^{-3}$, which is a typical density in these experiments. It was shown that the window of ions that noticeably contribute includes from Xe $^{+0}$ to Xe $^{+11}$, and therefore, the bound-bound contribution to the radiative properties will be the dominant one due to the abundance of the less ionized ions of Xe. This fact is well illustrated in Figure 1 where we have plotted the monochromatic opacity and emissivity for a density of matter 5×10^{-4} gcm $^{-3}$ and an electron temperature of 10 eV.

In Ryutov et al. [1] the conditions to define an optically thin, radiative regime for laboratory astrophysics experiments relevant to supernova remnants were formulated. In particular, in order to be optically thin the radiative flux should escape from the blast wave which implies that the photon mean free path, λ_{rad}, which is related to the mean opacity, must be larger than a characteristic size scale of the system, h. Furthermore, to be radiative, the radiative cooling time, τ_{rad}, which depends on the radiative power loss, must be shorter than the convective transport time, $\tau_{conv} = h/s$, with s the plasma sound speed. In Ref. [16] an analysis was carried out of blast waves launched in clusters that have typical gas densities around 5×10^{-4} gcm $^{-3}$ and post-shock temperatures around $5 - 10$ eV. For $h = 0.01$ cm Symes et al. [16] concluded that the plasma was optically thin and radiative. However, their calculation of the photon mean free path only included the bremsstrahlung contribution to the opacity that is not a good approximation at these low densities and temperatures where, due to the low ionization, line radiation is dominant. Furthermore, in their calculation of the

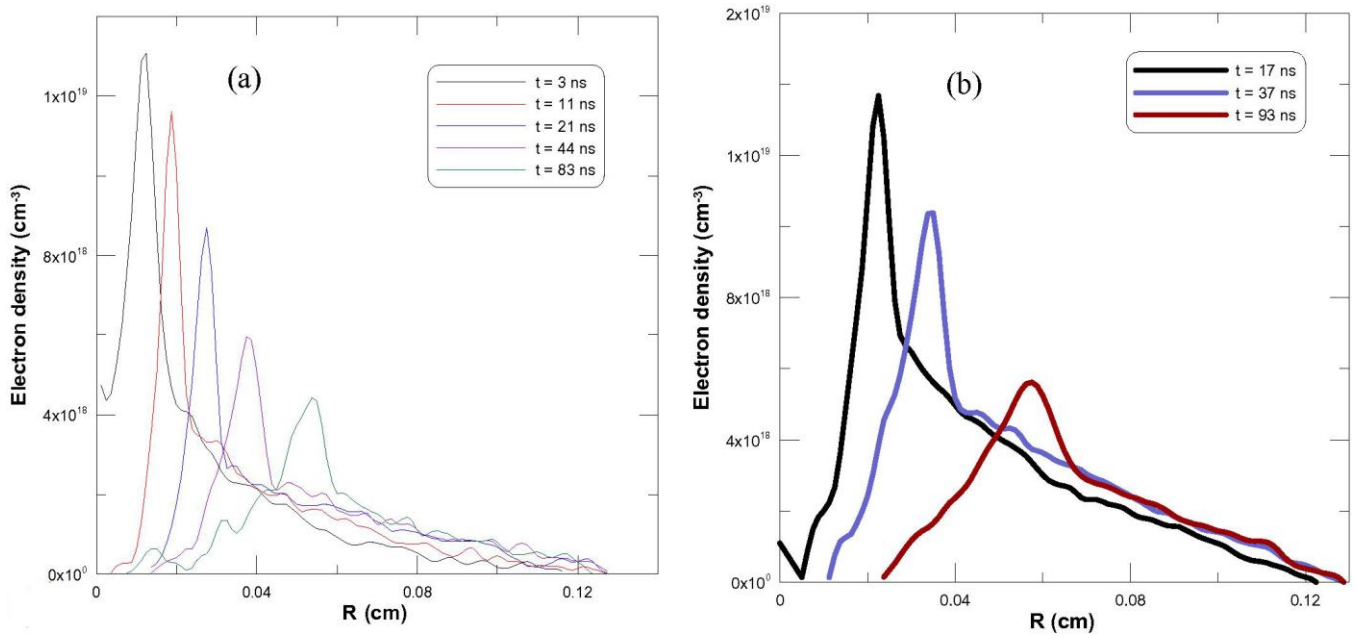

Figure 2. Structure of the radiative blast waves as a function of the time. (a) lower density and (b) higher density cases.

cooling time they used the cooling functions, i.e. the ratio between the radiative power loss and the electron and ion number densities, tabulated in Post et al. [17] which are obtained assuming Coronal equilibrium and therefore they are density-independent and are only accurate for electron densities lower than those obtained in the experiments of interest here. In [33] we performed these analysis using RAPCAL code. We calculated both the Rosseland and Planck mean free paths including the bound-bound and bound-free contribution and we found that, for a given temperature, the region where the plasma can be assumed optically thin is shifted with respect to the results showed in [16], toward lower densities due to the increase of the opacity from line absorption. In any case, we obtained that for the plasma conditions involved in this kind of experiments the mean free paths were always larger than h and, therefore, we concluded that the plasma in the post shock region could be assumed as optically thin. It is worth pointing out that this is an average comparison and, in fact, in some ranges of photon energies (10-40 and 60-100 eV), the plasma absorbs radiation as it is shown in [33] where it was compared the monochromatic photon mean path with h. However for almost the whole range of photon energies it can be assumed optically thin, and that confirms that this blast wave can be classified as thin-thin [8] as both the upstream and downstream media are optically thin. With respect to the radiative character of these blast waves, in [33] we performed a calculation of the cooling times for electron temperatures ranged between 1-20 eV and several of the typical matter densities in these experiments. In this case, the cooling functions were obtained using the CRSS implemented in ABAKO and, therefore, unlike the ones provided by Post et al. [17], they are valid in the plasma conditions under analysis. The comparisons between the cooling and convective times in [33] resulted in the former was always lower than the latter, which confirmed that the blast waves could be categorized as radiative.

3.2. Diagnostics of the radiative shock temperature

In this subsection we employ the study made of the average ionization as a function of the density and temperature to perform a diagnostics of the electron temperatures of cylindrical radiative blast waves launched in xenon using the THOR laser system at the University of Texas [15]. The gas of xenon clusters was irradiated with laser pulses of 35 fs duration with ≈ 440 mJ pulse energy at average gas density of 1.6×10^{-4} gcm $^{-3}$ and with ≈ 360 mJ per pulse for an average gas density of 2.5×10^{-4} gcm $^{-3}$. The blast waves formed were characterized using time-resolved transverse interferometric and Schlieren imaging. A detailed description of the experiment can be found in [15, 16]. Figure 2 shows typical electron density profiles for xenon blast waves produced during these experiments at several times for the two matter densities. From the Figures radiative precursors are detected ahead of the shock front. The average ionization values of pre-shock region are direct measurements from the interferograms since the ambient density of gas is known. Behind the shock the electron density is also experimentally measured and the average ionization is calculated assuming a shell compression, defined as the ratio of the maximum mass density within the shell to the ambient gas density ($c = \rho_{shell}/\rho_{ambient}$), equals to 2 [15]. This value for the compression was obtained from the ratio of the shell thickness to the shock front radius. This weak compression is because of the preheating of the gas ahead of the shock that reduces the Mach number [16]. However, the plasma temperature could not be experimentally measured. This was estimated in Ref. [16] making use of an approximate formula [13] derived from the Saha equation and thus assumes LTE. However LTE regime cannot be always assumed and therefore this estimation of the temperature could be not accurate enough and that could give, for example, unphysical solutions in the calculation of the compression ratio [16]. Our study of the average ionization provided us this quantity both in LTE and NLTE regimes and, therefore, our numerical simulations could give us an idea about the accuracy of the LTE estimation of the electron temperatures of the blast waves. Our procedure has been to search the electron temperature that at the electron density given experimentally, matches with the experimental average ionization, within a margin of error imposed.

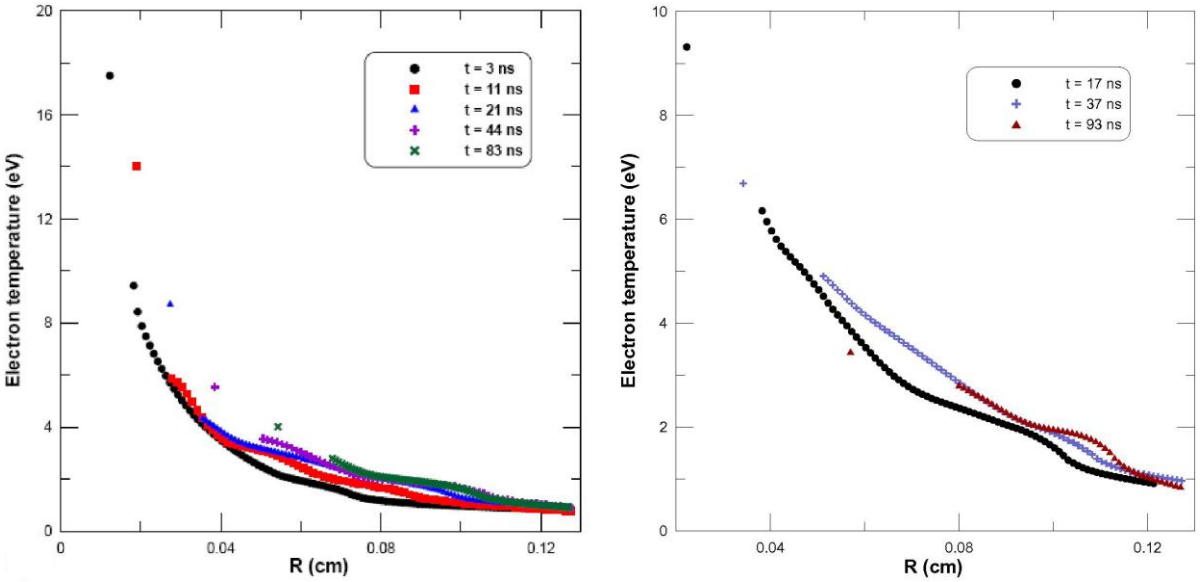

Figure 3. CRSS estimation of the electron temperature of both the shock front and the radiative precursor for several times.

However, as it was before commented, the calculation of the average ionization in NLTE regime entails large computational costs, since we have to solve a large set of rate equations. Therefore, in order to obtain the average ionization of the plasma at any couple of electron density and temperature we have carried out a fitting of this quantity to an analytical expression depending on these parameters. The data employed for the fittings are those provided by ABAKO calculations and the analytical expression employed for the fitting is given by

$$\log\overline{Z}(n_e, T_e) = \sum_{i=0}^{n} \sum_{j=0}^{m} C_{ij} (\log n_e)^i (\log T_e)^j. \quad (3)$$

The coefficients of the fitting, C_{ij}, are determined by means of a Least Squares Regression. We have imposed a relative error of 1%. The maximum degree of the polynomial both in electron temperature and density was fixed to 7 in order to avoid oscillating behaviors. In general, it is impossible to find only one polynomial function to make the fit of the whole range of plasma conditions and this one must be divided into subsets to obtain a polynomial fitting in each subset. In this case, for the range of plasma conditions of interest in this work, the number of polynomial functions required has been 4. Finally, in order to optimize the search of the subsets of plasmas conditions and the corresponding polynomial functions a quad-tree algorithm was used. In Figure 3 the estimation of the temperatures of the blast waves, at both densities, are shown for the different times considered in Figure 2. In Figure 3 the largest value of the electron temperature for each time corresponds to the greatest value of the electron density, at each time, in Figure 2. This temperature is assumed as the shock front temperature. The other temperatures represented correspond to points belonging to the radiative precursor. Due to the power delivered by the laser to the xenon cluster it is estimated that the largest electron temperature reached in the plasma is around 20 eV and the electron temperatures obtained with our CRSS model fulfill that condition.

From the Figures we observe that the temperature of the shock front decays with the time which is expected due to the radiative cooling. We also detect that for those points of the radiative precursor far from the shock front the temperature is almost time independent. Due to the fast variation of the electron temperature of the shock front, overall at early times, one could ask whether the stationary approach in the CRSS model is accurate for the kinetics calculations. As it is known, a plasma can be assumed in stationary state when the characteristic time of the dominant atomic process, τ_a, calculated from the cross section of that process, is much smaller than the plasma characteristic time, t_{plasma}, given by

$$\tau_{plasma} = \left| \frac{T_e}{\partial T_e / \partial t} \right|. \quad (4)$$

For the shock front, this condition is not verified since due to the strong cooling the temperature of the shock front changes with time faster than the characteristic time. On the other hand, since the radiative precursor precedes the shock by as much as 800 μm [15] the time scale for the precursor to reach a steady state is about 40 ns [42]. Therefore, the estimation of the electron temperatures presented in this work, overall for times shorter than 40 ns, could change if a time-dependent kinetics calculation of them is performed and in a future work it is our purpose to carry out a time-dependent collisional-radiative calculation of the radiative properties and the electron temperatures of the blast wave of this experiment in order to quantify the time effects. In any case, this CRSS estimation of the temperatures is useful in order to analyze the accuracy of their LTE calculations, since this assumption is very common for their calculation, as in Symes et al. [16].

In Figures 4 and 5 we have represented the behavior of the shock front temperature and radiative power loss with time for both matter densities of the experiment. Furthermore, in those figures we perform a comparison of calculations of them using the CRSS model and Saha-Boltzmann (SB) equations, i.e. assuming LTE. We detect that for the case of lower density the temperatures estimated by both calculations show some differences, overall at early times. Thus, for example, at 3 ns the CRSS and SB calculations of the temperature give 17.38 and 16.20 eV, respectively, i.e. a

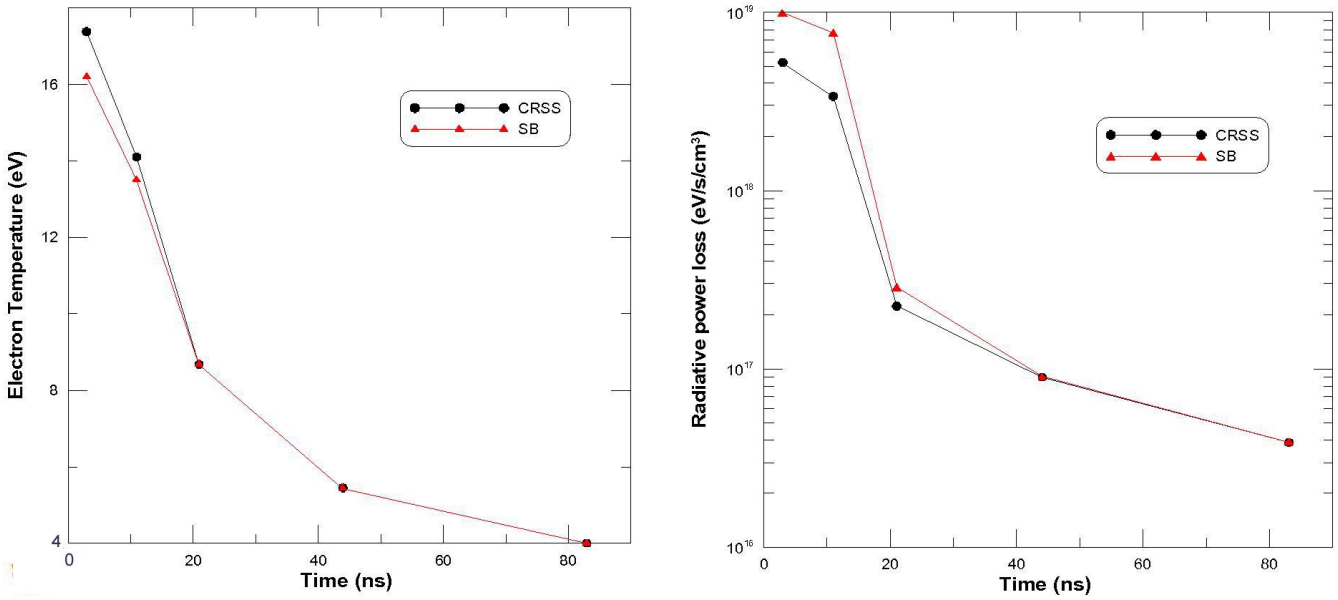

Figure 4. Comparison between CRSS and Saha-Boltzmann (SB) calculations of the shock temperatures (left) and radiative power losses (right) as a function of time.

relative difference about 7.3%. These differences decrease with time and for times later than 20 ns both models provide almost the same shock temperature, which means that the average ionization is also quite similar. On the other hand, for the higher density case both calculations provide very similar average ionization and, therefore, shock electron temperatures and for this reason in Figure 5 we have only shown the CRSS calculation of the temperature. From the figures we observe that for a given time the shock front temperature is greater for the higher density situation than for the lower density. In Figures 4 and 5 we have also represented the radiative power loss from the shock shell, a key magnitude in radiative shocks. We can observe that for a given time the radiative power loss for the higher density case is always larger than for the lower density case due to the temperature also greater. Furthermore, we have also made a comparison between CRSS and SB simulations of this quantity. In both densities some differences are appreciable although they are greater in the lower density case. Thus, for example, around 20 ns the difference is about 80% whereas for the higher density is about 50%. We have checked that both simulations provide almost the same CSDs and, therefore, average ionization and electron temperatures, but the atomic levels, overall the excited ones, cannot be assumed in LTE and this is the reason of the discrepancy in the radiative power losses at this time. Only at the last times, i.e later than 80 ns, the differences are lower than 10% and then a LTE simulation of the radiative power loss could be accurate enough.

In the previous section it was established that the blast wave could be classified as thin-thin and radiative. The analysis was made for a typical plasma condition in this kind of experiments. Once we have estimated the electron temperatures under these assumptions we have checked them. If the plasma is optically thick, the set of the rate equations 1 must be solved together with the radiative transfer equation,

$$\frac{1}{c}\frac{\partial I(\mathbf{r},t,\nu,\mathbf{e})}{\partial t} + \mathbf{e}\cdot\nabla I(\mathbf{r},t,\nu,\mathbf{e}) = -\kappa(\mathbf{r},t,\nu)I(\mathbf{r},t,\nu,\mathbf{e}) + j(\mathbf{r},t,\nu), \quad (5)$$

where I is the specific intensity, $\mathbf{r}$ is the position vector and $\mathbf{e}$ a unitary vector in the direction of the radiation propagation. The emissivity and the absorption coefficient couple the radiative equation with the rate equations. In ABAKO stationary conditions are assumed for the radiative transfer and, therefore, the first sum in the left hand of Equation (5) equals zero. In the current version of ABAKO only bound-bound opacity effects are taken into account [20]. These ones are included in an approximate way by means of the escape factor formalism which avoids the explicit solution of the radiative transfer equation. To compute the escape factors we have adopted the technique described in [43]. This formalism avoids the need to perform a simultaneous calculation of radiation transport and atomic physics. We have made kinetics calculations of the shock shell of the blast wave including plasma opacity effects assuming that the plasma in the shock shell is homogeneous, with cylindrical geometry being the radius equals to its full width at half maximum (FWHM). For the situation of higher density, the electron temperatures obtained including opacity effects in the kinetics calculations are almost identical to the ones obtained without including them. As it was shown before, for the higher density CRSS and SB calculations provide the same average ionizations and electron temperatures, and, therefore, in steady-state situations, the plasma could be assumed in LTE. Since in this regime the collisional processes dominate, opacity effects do not introduce appreciable changes in the plasma level populations. On the other hand, for the case of lower density, the electron temperature calculated at 3 ns including opacity effects is 16.30 eV, whereas without that effects was 17.38 eV and assuming LTE was 16.20 eV. As expected, the opacity effects lead the plasma to LTE regime. At 11 ns the the electron temperatures obtained with or without opacity effects are 13.70 and 14 eV, respectively, and at 21 ns the temperatures are almost identical. Therefore, only at 3 ns an optically thick calculation of the plasma level populations introduce differences in the electron temperature estimation. However, this difference is overestimated since we have assumed that for the whole FWHM of the shock shell the

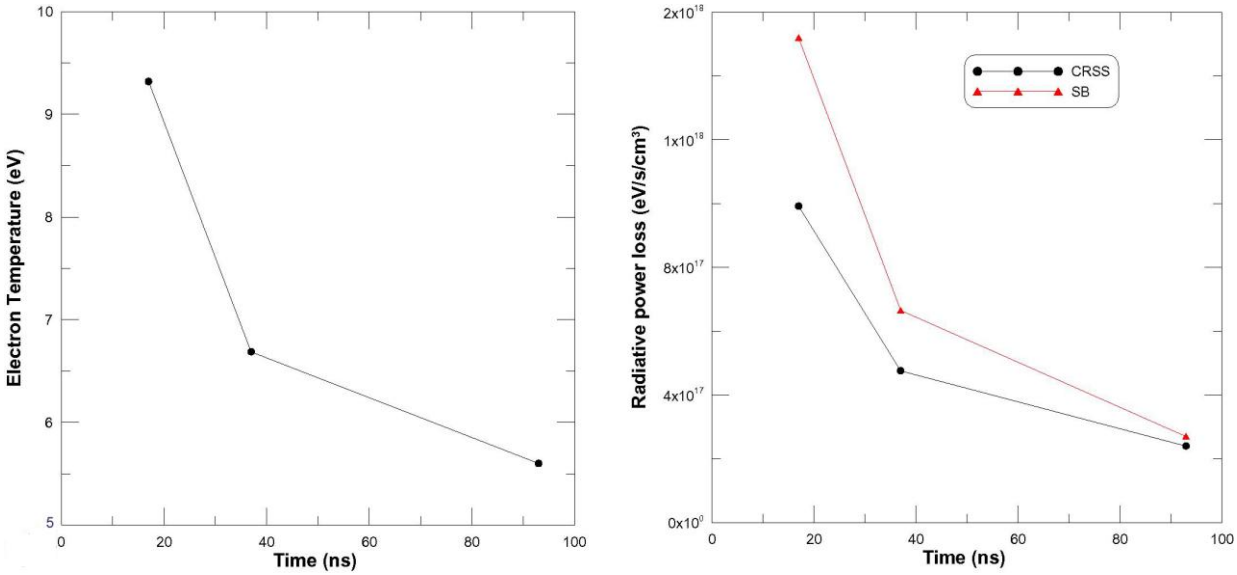

Figure 5. Shock temperatures (left) and radiative power losses (right) as a function of time.

electron densities and temperatures have their maximum values, which is not true. Therefore, we could conclude that, in general, opacity effects do not change appreciably the kinetics calculations and the shock shell can be considered as optically thin.

Finally, we have also compared the radiative cooling time of the blast wave with the convective time. To calculate the latter we have assumed as the temperature of the gas ahead of the shock front the highest one of the radiative precursor and, therefore, we are underestimating the convective transport time. Even so, we have obtained, for both densities and all the electron temperatures diagnosed, that the radiative cooling time ($\approx 10^{-10}$ s) is considerably shorter than the convective time ($\approx 10^{-5}$ s), which agrees with the fact that the blast wave can be considered as radiative.

4. Conclusions

In this work we have analyzed the radiative character of blast waves launched in clusters of xenon, which are generated to reproduce in laboratory supernova remnants. We have proved that these experimental blast waves are optically thin by comparing the photon mean free path with the characteristic size of the systems and making a collisional-radiative simulation including self-absorption effects as well. Furthermore, for a given experiment, where the plasma electron temperatures are not experimentally measured, we have made a diagnostics of the temperature by means of collsional-radiative simulations. These simulations were made assuming stationary state but we have found that for the early times of the radiative blast wave a time-dependent simulation could be required.

Acknowledgements

This work has been supported by the Research Project of the Spanish Government ((ENE2009-11208/FTN), and also by the Keep in touch Project of the European Union.

References

1. D. Ryutov, R. P. Drake, J. Kane, B. A. Remington and W. M. Wood-Vasey, Astrophys. J. 518 (1999) 821.
2. D. Ryutov, R. P. Drake and B. A. Remington, Astrophys. J. Suppl. Ser. 127 (2000) 465.
3. B. A. Remington, R. P. Drake and D. Ryutov, Rev. Mod. Phys. 78 (2006) 755.
4. J. I. Castor, Astrophys. Space Sci. 307 (2007) 207.
5. E. Falize, S. Bouquet and C. Michaut, Astrophys. Space Sci. 322 (2009) 107.
6. S Bouquet, E. Falize, C. Michault, C. D. Gregory, B. Loupias, T. Vinci and M. Koenig, High Energy Density Phys. 6 (2010) 368.
7. A. S. Moore, J. Lazarus, M. Hohenberger, J. S. Robinson, E. T. Grumbell, M. Dunne and R. A. Smith, Astrophys. Space Sci. 307 (2007) 139.
8. R. P. Drake, High Energy Density Physics, Springer-Verlag, Berlin (2005).
9. M. Gonzalez, C. Stehle, E. Audit, M. Busquet, B. Rus, F. Thais, O. Acef, P. Barroso, A. Bar-Shalom, D. Baudin, M. Kozlova, T. Lery, A. Madouri, T. Mocek and J. Polan, Laser Part. Beams 24 (2006) 535.
10. M. Busquet, E. Audit, M. Gonzalez, C. Stehle, F. Thais, O. Acef, D. Bauduin, P. Barroso, B. Rus, M. Kozlova, J. Polan and T. Mocek, High Energy Density Phys. 3 (2007) 8.
11. C. Stehle, A. Ciardi, J. P. Colombier, M. Gonzalez, T. Lanz, A. Marocchino, M. Kozlova and B. Rus, Laser Part. Beams 27 (2009) 709.
12. J. Lindl, Phys. Plasmas 2 (1995) 3933.
13. R. P. Drake and A. B. Reighard, In: Proceedings of the Conference of the APS Topical Group On Shock Compression Of Condensed Matter, American Physical Society, Vol. 845 (2006) p. 1417.
14. D. R. Bates, A. E. Kingston and R. W. McWhirter, Proc. R. Soc. London Ser. A 267 (1962) 297.
15. J. Osterhoff, D. R. Symes, A. D. Edens, A. S. Moore, E. Hellewell and T. Ditmire, New J. Phys. 11 (2009) 023022.
16. D. R. Symes, M. Hohenberger, J. Lazarus, J. Osterhoff, A. S. Moore, R. R. Faustlin, A. D. Edens, H. W. Doyle, R. E. Carley, A. Marocchino, J. P. Chittenden, A. C. Bernstein, E. T. Gumbrell, M. Dunne, R. A. Smith and T. Ditmire, High Energy Density Phys. 6 (2010) 274.

17. D. E. Post, R. V. Jensen, C. B. Tarter, W. H. Gransberger and W. A. Lokke, Atom. Data Nucl. Data 20 (1977) 397.
18. K. B. Fournier, M. Cohen, M. J. May and W. H. Goldstein, Atom. Data Nucl. Data 70 (1998) 231.
19. K. B. Fournier, M. J. May, D. Pacella, M. Finkenthal, B. C. Gregory and W. H. Goldstein, Nucl. Fusion 40 (2000) 847.
20. R. Florido, R. Rodriguez, J. M. Gil, J. G. Rubiano, P. Martel, E. Minguez and R. C. Mancini, Phys. Rev. E. 80 (2009) 056402.
21. R. Rodriguez, R. Florido, J. M. Gil, J. G. Rubiano, D. Suarez, P. Martel, E. Minguez and R. C. Mancini, Commun. Comput. Phys. 8 (2010) 185.
22. C. Bowen, R. W. Lee and Yu. Ralchenko, J. Quant. Spectrosc. Radiat. Transfer 99 (2006) 102.
23. J. G. Rubiano, R. Florido, C. Bowen, R. W. Lee and Yu. Ralchenko, High Energy Density Phys. 3 (2007) 225.
24. C. J. Fontes, J. Abdallah, C. Bowen, R. W. Lee and Yu. Ralchenko, High Energy Density Phys. 5 (2009) 15.
25. W. Lotz, Z. Phys. 206 (1967) 205.
26. H. V. Van Regemorter, Astrophys. J. 136 (1962) 906.
27. H. A. Kramers, Philos. Mag. 46 (1923) 836.
28. H. R. Griem, Principles of plasma spectroscopy, Cambridge University Press, Cambridge (1997).
29. M. F. GU, Can. J. Phys. 86 (2008) 675.
30. J. C. Stewart and K. D. Pyatt, Astrophys. J. 144 (1966) 1203.
31. O. Peyrusse, C. Bauche-Arnoult and J. Bauche, Phys. Plasmas 12 (2005) 063302.
32. S. Hansen, J. Bauche, C. Bauche-Arnoult and M. F. Gu, High Energy Dens. Phys. 3 (2007) 109.
33. R. Rodriguez, J. M. Gil, G. Espinosa, R. Florido, J. G. Rubiano, M. A. Mendoza, P. Martel, E. Minguez, D. R. Symes, M. Hohenberger, R. A. Smith, Plasma Phys. Control. Fusion 54 (2012) 045012.
34. R. Rodriguez, R. Florido, J. M. Gil, J. G. Rubiano, P. Martel and E. Minguez, Laser Part. Beams 26 (2008) 433.
35. D. Mihalas, Stellar Atmospheres, Freeman, San Francisco (1978).
36. M. S. Dimitrijevic and N. Konjevic, Astron. Astrophys. 172 (1987) 345.
37. J. Bauche, C. Bauche-Arnoult and M. Klapisch, Adv. Atom. Mol. Phys. 23 (1987) 131.
38. S. J. Rose, J. Phys. B 25 (1992) 1667.
39. R. J. Rutten, Radiative Transfer in Stellar Atmospheres, Utretch University Lectures Notes (8th ed.), Utretch (2003).
40. F. J. D. Serduke, E. Minguez, S. J. Davidson and C. A. Iglesias, J. Quant. Spectrosc. Radiat. Transfer 65 (2000) 527.
41. H. K. Chung, K. B. Fournier and R. W. Lee, High Energy Density Phys. 2 (2006) 7.
42. R. P. Drake, Astrophys. Space Sci. 298 (2005) 49.
43. R. C. Mancini, R. F. Joyce, C. F. Hooper Jr., J. Phys. B 20 (1987) 2975.

R. Rodriguez *et al.*: **Determination and analysis of plasma radiative properties for numerical simulations of laboratory radiative blast waves launched in xenon clusters.** *J. Spectrosc. Dyn.* 2013, **3:** 17